



Aerodynamic Characteristics Over Fine-Grained Gravel Surfaces in a Wind Tunnel

Jiaqi Liu*, Reiji Kimura and Jing Wu

Arid Land Research Center, Tottori University, Tottori, Japan

OPEN ACCESS

Edited by:

Liguang Wu,
Fudan University, China

Reviewed by:

Jiqiang Niu,
Southwest Jiaotong University, China
Qingyuan Liu,
Chinese Academy of Meteorological
Sciences, China

*Correspondence:

Jiaqi Liu
ryuu731@tottori-u.ac.jp

Specialty section:

This article was submitted to
Atmospheric Science,
a section of the journal
Frontiers in Earth Science

Received: 21 September 2021

Accepted: 04 November 2021

Published: 23 November 2021

Citation:

Liu J, Kimura R and Wu J (2021)
Aerodynamic Characteristics Over
Fine-Grained Gravel Surfaces in a
Wind Tunnel.
Front. Earth Sci. 9:758910.
doi: 10.3389/feart.2021.758910

Gravels can protect soil from wind erosion, however, there is little known about the effects of fine-grained gravel on aerodynamic characteristics of the near-surface airflow. Drag coefficient, wind-speed gradient, and turbulent transfer coefficient over different coverages of gravel surfaces were investigated in a compact boundary-layer wind tunnel. The drag coefficient of the fine-grained gravel surface reached the maximum value at 15% coverage and then tended to stabilize at gravel coverage 20% and greater. At a height of 4 cm, near-surface airflow on gravel surfaces can be divided clearly into upper and lower sublayers, defined as the inertial and roughness sublayers, respectively. The coefficient of variation of wind speed over gravel surfaces in the roughness sublayer was 8.6 times that in the inertial sublayer, indicating a greater effect of gravel coverage on wind-speed fluctuations in the lower layer. At a height of 4 cm, wind-speed fluctuations under the observed wind speeds were independent of changes in gravel coverage. In addition, an energy-exchange region, where sand particles can absorb more energy from the surrounding airflow, was found between the roughness and inertial sublayers, enhancing the erosional state of wind-blown sand. This finding can be applied to evaluate the aerodynamic stability of the gravel surface in the Gobi Desert and provide a theoretical basis for elucidation of the vertical distributions of wind-blown sand flux.

Keywords: arid regions, drag coefficient, gravel coverage, turbulent transfer coefficient, wind-speed gradient

INTRODUCTION

The Gobi Desert is one of the primary geomorphological types widely distributed in arid and semi-arid regions of Mongolia and northern China. It is also one of the main sources of Asian Dust that results from wind erosion (Bian et al., 2011). During the development of the gobi surface, erodible materials (mainly sand grains) gradually decreased because of long-term wind erosion, whereas non-erodible materials (mainly gravel) remained, forming a non-erodible gravel layer that protects the underlying deposits from further erosion (Bagnold, 2012). The inhibiting effect of this gravel surface on wind erosion and wind-blown sand has been studied widely (Zhang et al., 2014; Liu and Kimura, 2018; Liu et al., 2020). Liu and Kimura (2018) pointed out that most sand particles were trapped at 15% coverage of fine-grained gravel on the surface. In a study of aeolian processes over the great gravel surface at Mogao Grottoes, Zhang et al. (2014) suggested that the surface was protected from wind erosion most effectively at an artificial gobi surface with 30% gravel coverage. They also found that the characteristics of aeolian processes changed from aeolian to depositional as gravel coverage increased. Liu et al. (2020) examined blown sand flux over fine-grained gravel surfaces and reported an erosional state at all experimental coverages. However, it is imperfectly known how and to what

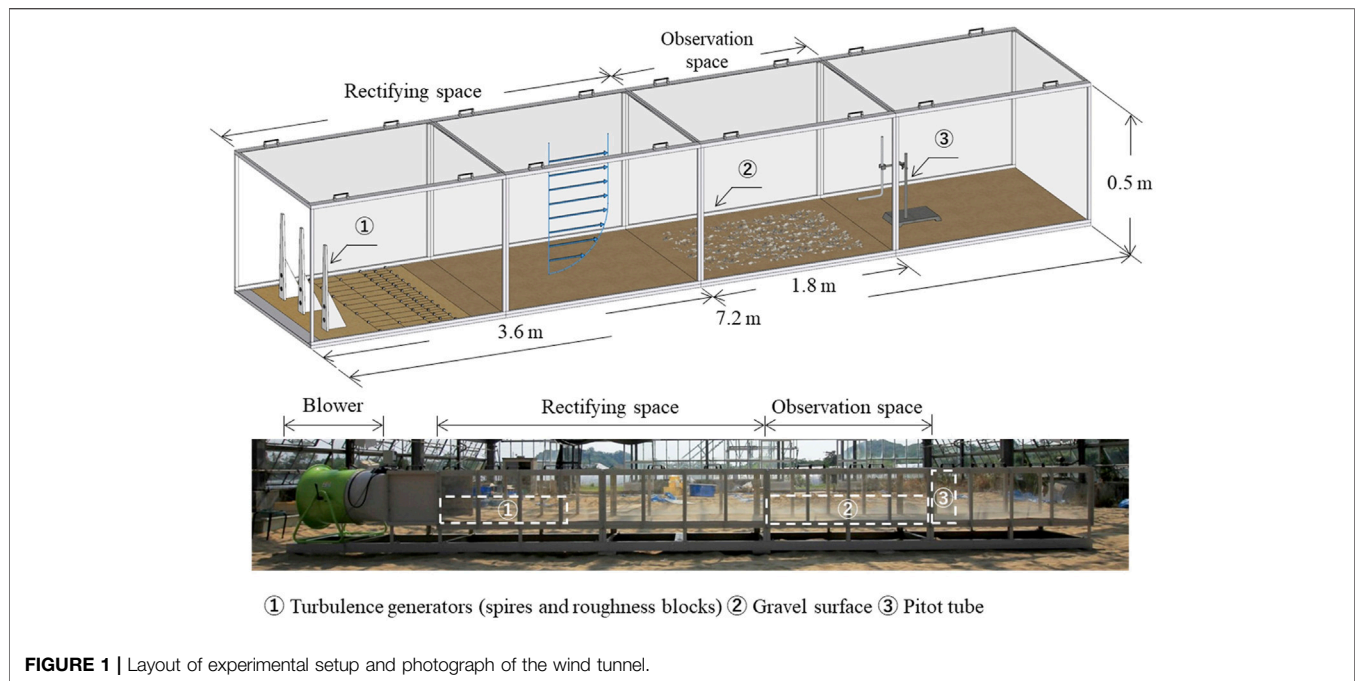


FIGURE 1 | Layout of experimental setup and photograph of the wind tunnel.

extent aerodynamic characteristics of airflow over gravel surfaces affect the transition between aeolian and depositional regimes.

Parameters related to wind profiles, such as drag coefficient, wind-speed gradients, and turbulent transfer coefficient, have been developed to evaluate aerodynamic characteristics of airflow near the ground surface (Dong Z. B. et al., 2002). The dimensionless drag coefficient reflects the drag force generated by obstacles in airflow; this coefficient can be applied to assess the wind-blown sand and dust emission potential of gravel surfaces and hence the aerodynamic stability (Dong Z. et al., 2002). In addition, airflow intensity on gravel surfaces can be characterized by wind-speed gradients with height. As one of the important roughness elements, gravels reduce wind velocity (shear stress) by absorbing part of the wind momentum, thus suppressing wind erosion through their drag effect on airflow in the boundary layer (Marticorena et al., 1997). In wind-erosion studies, sand transport is determined by the momentum transfer in the near-ground surface layer. The capacity of airflow to transfer momentum for a given gradient of wind can be expressed by the turbulent transfer coefficient, which represents the intensity of energy exchange in the vertical direction and hence affects the structural characteristics of wind-blown sand (Shao, 2008). Therefore, understanding the aerodynamic characteristics of the near-surface airflow is important for controlling wind erosion.

The drag coefficient, wind-speed gradient, and turbulent transfer coefficient can be measured by field observations or wind tunnel experiments. Field observations provide validation data for simulations, although the variables cannot be controlled. Because those variables are related not only to geometric characteristics of roughness elements (such as size and shape of gravel) but also to natural

topography, such uncontrolled conditions lead to difficulties in interpreting field observations. In contrast, in a wind tunnel, parameters are adjustable for specific experimental conditions (Shao, 2008). In realistic modeling, however, the atmospheric boundary layer restricts quantitative research on aerodynamic characteristics of near-surface airflow. In wind tunnel experiments, (Tan et al., 2013) found that the best gravel coverages for reducing wind speed for gravels with diameters of 2, 3, and 5 cm were 25, 35, and 20%, respectively. However, few studies have been done on variations in wind-reduction effect with height above fine-grained gravel surfaces (diameter <10 mm), which is typical in the Mongolian Gobi Desert.

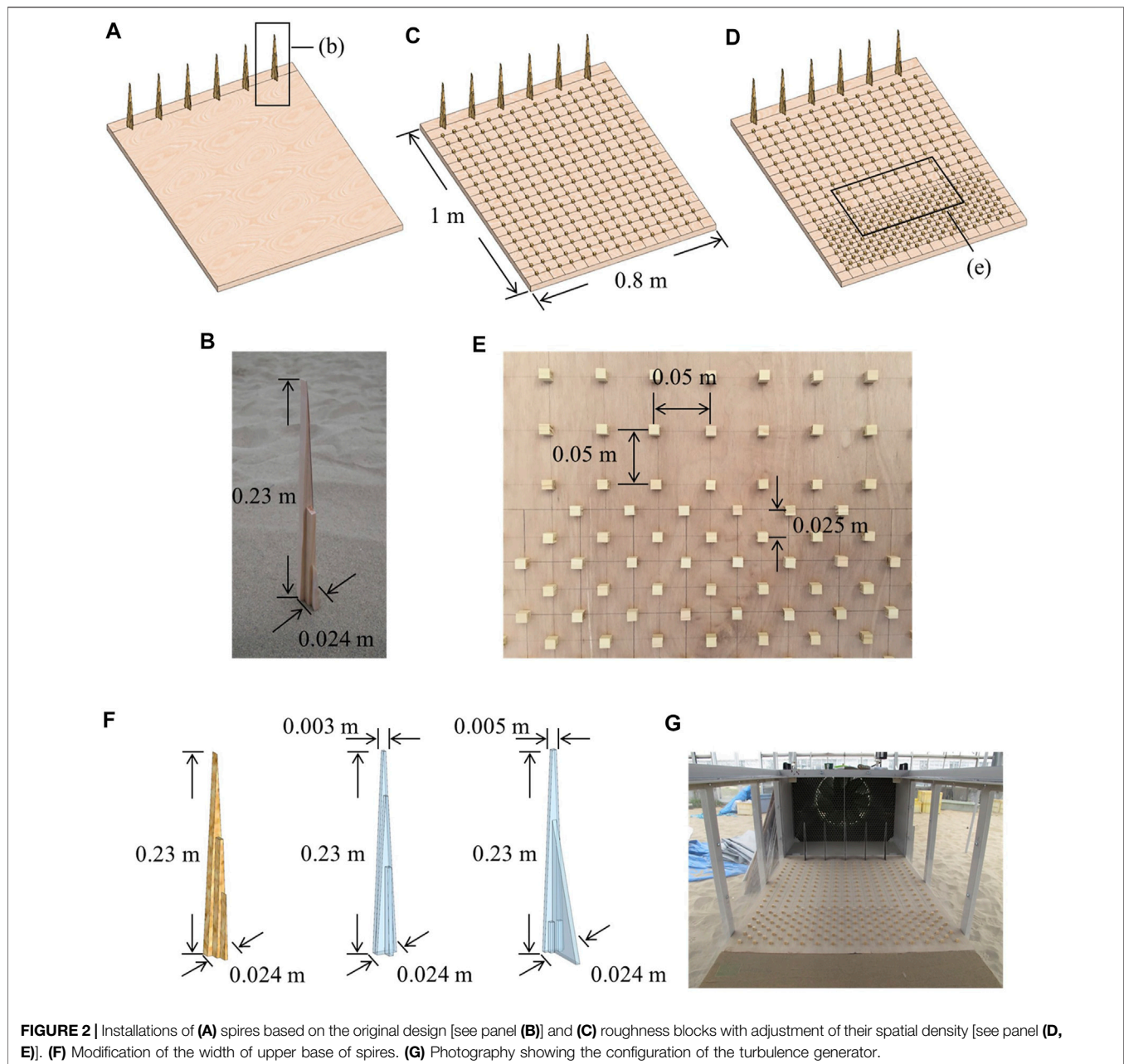
To clarify the effects of gravel surfaces on aeolian transport, we compared the influence of gravel coverage on the drag coefficient, wind-speed gradient, and turbulent transfer coefficient in a compact boundary-layer wind tunnel developed by Liu and Kimura (2017a, 2017b).

MATERIALS AND METHODS

Experimental Setup of Wind Tunnel

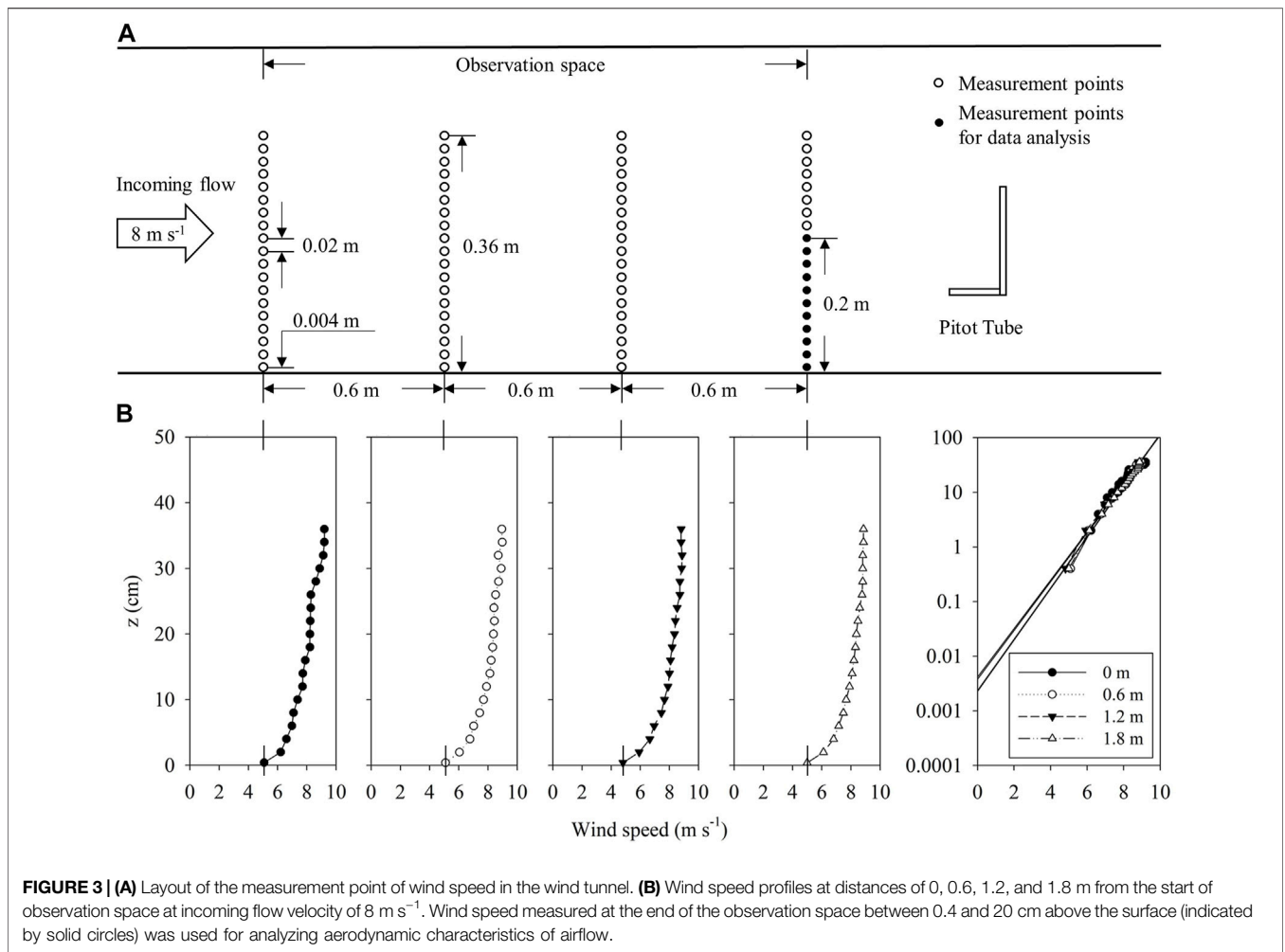
We conducted experiments in a small-scale, open-circuit wind tunnel (Figure 1) at the Arid Land Research Center at Tottori University, Japan. The wind tunnel was 8.25 m long, had a 0.8 m × 0.5 m cross section, and could generate airflow speeds of up to 12 m s⁻¹, controlled by adjustment of a power inverter. Wind speeds were measured with a pitot tube at a height of 20 cm downwind side of the observation space.

To ensure experimental conditions in the wind tunnel can reasonably represent those occurring in the natural



environment, we designed turbulence generators comprising spires and roughness blocks. We firstly calculated the dimensions of the triangular spires and roughness blocks based on the empirical formulas determined by Irwin (1981) (**Figures 2A–C**). The use of spires enabled us to generate a boundary layer. More than 90% wind-blown sand movement (mainly saltation) occurs within 30 cm of the surface (Butterfield, 1999; Shao, 2008). By modifying the width of the upper base of the spires without changing their height or base-width (**Figure 2F**), the wind tunnel produced a

boundary layer 34 cm thick, which satisfies the requirement of greater than 30 cm. The use of modified trapezoidal spires also enabled as to achieve an increased roughness length. The wind profiles and turbulence characteristics can be adjusted by arranging the numbers of spires (Niu et al., 2017) and the spatial density of roughness blocks (Liu and Kimura, 2017b). The method was used to obtain uniform distributions of horizontal wind speed in this study (**Figures 2C–E**). A group of spires and roughness blocks was installed between the blower and the sand bed (**Figure 2G**) (Liu and Kimura,



2017a). As a result, this system generated a thick boundary layer (34 cm high) over the sand bed, a roughness length of 0.003 ± 0.0007 cm close to that of the natural field environment (Darmenova et al., 2009), and uniform distributions of horizontal wind speed over the observation space.

We tested the vertical profiles of wind speeds at an incoming flow velocity of 8 m s⁻¹ along the centerline of the wind tunnel at 0.6 m intervals from the start of the observation space (Figure 3A). Wind speed was measured with a pitot-tube anemometer (MK Scientific DT 8920) fixed on a stand. The vertical wind speed profile was measured at 2-cm intervals between 0.4 and 36 cm above the sand surface. We obtained similar logarithmic distributions of vertical speeds and relatively uniform roughness length at the four measuring points in the observation space (Figure 3B).

Measurement of Wind Speed

To measure wind-speed characteristics, the floor of the wind tunnel was covered with a wooden board coated from the rectifying space to the observation space with sand from the

Tottori Sand Dune. The sand served to prevent damage to the anemometer by blown sand and to maintain a consistent surface roughness condition. The measurement of wind-speed characteristics requires the achievement of flow similarity in the wind tunnel (Jensen, 1958; Jensen and Franck, 1963), that is, the roughness parameter of the wind tunnel must be proportional to that in nature:

$$\frac{Z_0}{z_0} = \frac{D}{d}, \tag{1}$$

where Z_0 and z_0 are the roughness length in nature and wind tunnel, respectively, D and d are a dimension of the roughness elements in nature and wind tunnel, respectively. The turbulence generators in our wind tunnel generated a roughness length close to that of the natural environment. The gravel (i.e., roughness element), from the Tenryū River basin, was composed of pebbles 5–10 mm in diameter and defined as fine-grained gravel in our study (Friedman and Sanders, 1978), similar in size to gravel in southern Mongolia. Therefore, the airflow conditions can be simulated successfully in the wind tunnel. The gravel coverage

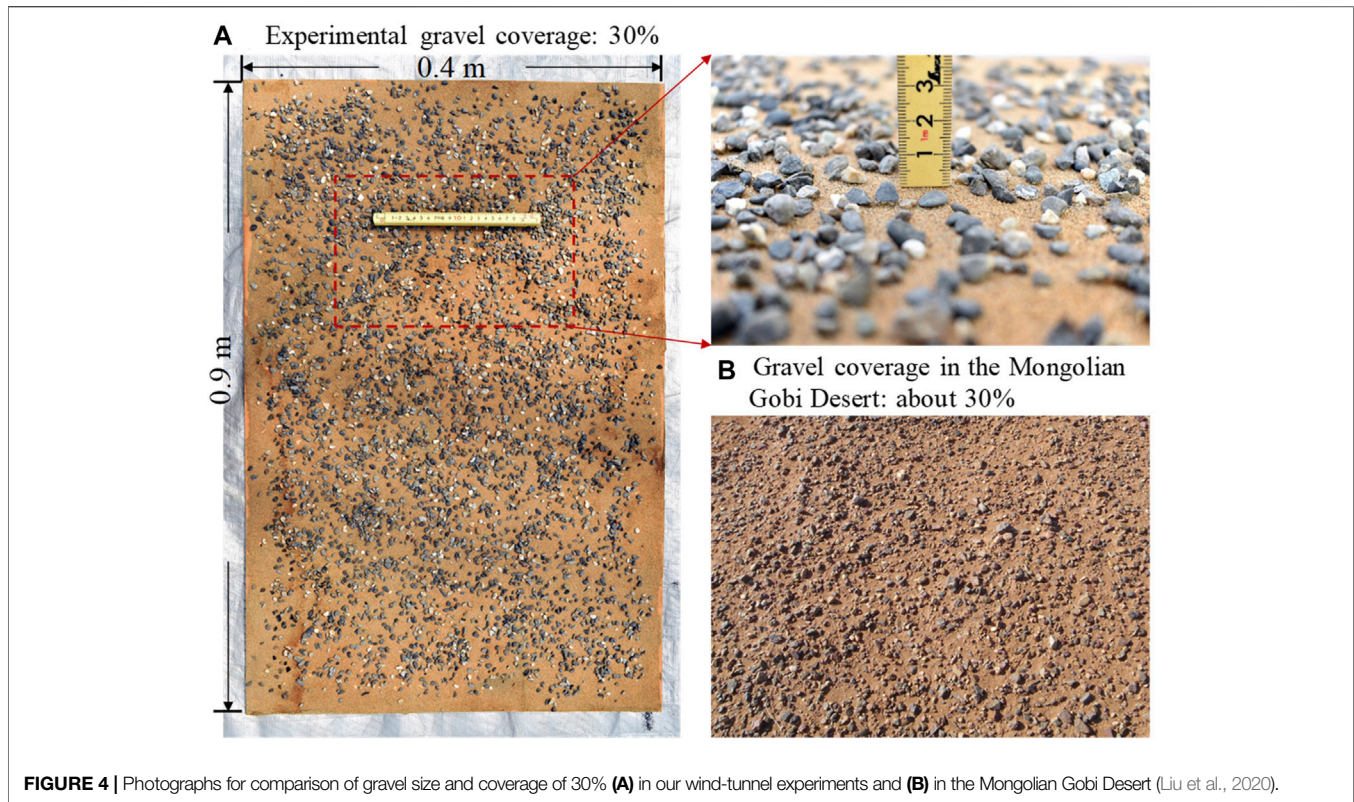


FIGURE 4 | Photographs for comparison of gravel size and coverage of 30% **(A)** in our wind-tunnel experiments and **(B)** in the Mongolian Gobi Desert (Liu et al., 2020).

was set at 5, 10, 15, 20, 25, and 30% by bonding an appropriate amount of gravel to sand-covered wooden boards that measured 0.4 m × 0.9 m. The flat sand surface without gravel was considered to be 0% coverage. Gravel coverage was determined by weight because we found after three trials that an average of 3.24 kg of gravel was needed to completely cover a board. Gravel coverage of 30%, requiring 0.97 kg of gravel, approximated the coverage of the actual dust-source region in southern Mongolia (**Figure 4**) (Liu et al., 2020).

We made experimental runs at wind speeds (incoming flow velocities) of 6, 8, and 10 m s⁻¹. The threshold wind speed for saltation was 6 m s⁻¹. The wind speed profile measured by a pitot-tube anemometer between 0.4 and 20 cm above the sand surface at the downwind end of the observation space was used for analysis (**Figure 3A**). The pitot-tube anemometer has an accuracy of ±2.5% at wind speed of 10 m s⁻¹. Wind speed was recorded at intervals of 1 s to a laptop connected with the device. We tested and obtained similar vertical profiles of wind speed using the average of 1-s measurements over 1, 3, 5, and 10 min. In this paper, the average of 60 readings (1-min average) was used for analysis.

The roughness length, an important parameter that affects airflow conditions, is the height at which wind speed is zero. For a homogeneous underlying surface, the roughness length can be calculated directly from observed data (Garratt, 1994). Assuming that the observed wind speed profile follows **Eq. 2** under atmospheric neutral conditions, roughness length and friction velocity are determined from observed wind speed profiles by using a computerized graphical procedure based on this equation.

$$u_z = \frac{u_*}{k} \ln \frac{z-d}{z_0}, \quad (2)$$

where u_z is wind speed at z cm above the sand surface, u_* is friction velocity (m s⁻¹), k is the von Karman's constant (= 0.4), d is the zero plane displacement (m), and z_0 is roughness length (cm). Zero plane displacement d can be neglected for the size of fine-grain gravel (Dong Z. B. et al., 2002). Then,

$$u_z = \frac{u_*}{k} \ln \frac{z}{z_0}, \quad (3)$$

Roughness length z_0 is obtained from the intercept of the plotted line on the vertical axis. The slope of each plotted line is the corresponding friction velocity $u_*/0.4$. We calculated u_* and z_0 at each gravel coverage.

Drag Coefficient

The drag coefficient is defined as the surface resistance to atmospheric flow. The relationship among drag coefficient, height, and roughness length in the surface layer is given by

$$C_{DN} = k^2 \left[\ln \left(\frac{z}{z_0} \right) \right]^{-2}, \quad (4)$$

where C_{DN} is the drag coefficient under atmospheric neutral conditions (Stull, 2012). Frank and Kocurek (1994) suggested that wind profiles and vertical structures of blown sand flux can be affected by atmospheric stability. In our wind tunnel experiment, however, the temperature change is small throughout the layer,

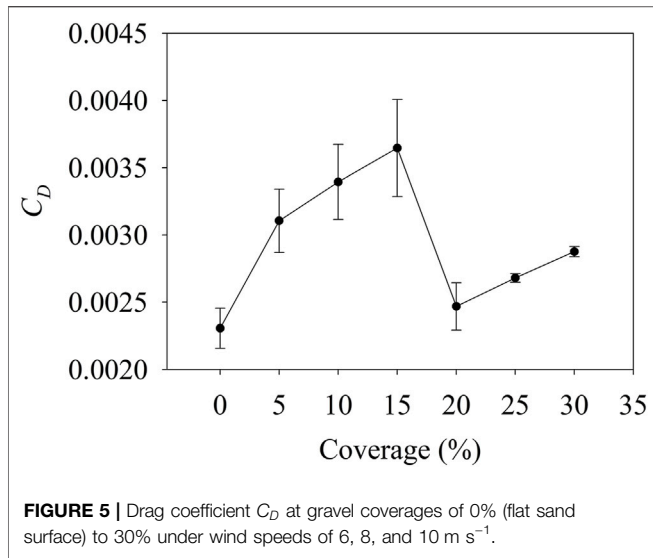


FIGURE 5 | Drag coefficient C_D at gravel coverages of 0% (flat sand surface) to 30% under wind speeds of 6, 8, and 10 m s⁻¹.

and the effects of atmospheric stability on wind profiles can be neglected. Then

$$C_D = C_{DN} = \left(\frac{u_*}{u_z}\right)^2, \tag{5}$$

where C_D is the drag coefficient. So C_D can be calculated by using u_* as a measure of surface stress associated with drag and u_z at 20 cm height which is the observation height of the incoming flow.

The variation of wind-speed gradient over gravel surfaces influences the wind-reduction effect and the inhibiting effect on blown sand flux through its impact on the structural characteristics of wind-blown sand. To quantify this variation, we used the coefficient of variation (CoV), which is a normalized measure of the dispersion of a distribution (Cosseron et al., 2013). Here, we employed CoV to evaluate the dispersion of wind speed distribution under different gravel coverages at each measured height. The coefficient of variation is defined as follows:

$$CoV = \frac{\sigma}{\mu}, \tag{6}$$

Here, μ is the mean of the wind speed and σ is the SD.

In the near-ground surface layer, the exchange and transmission of matter and energy are caused mainly by turbulence. This results in 80–90% of wind-blown sand particles being transported throughout this layer (e.g., Sharp, 1980). The turbulent momentum flux of each unit of time and area can be written as

$$\overline{u'w'} = -\frac{\tau}{\rho} = -u_*^2 \quad \text{viz.} \quad -\overline{u'w'} = u_*^2, \tag{7}$$

where τ is ground shear stress and ρ is air density. Following (Lu and Dong, 2006), we considered only the dynamical turbulence of neutral conditions and used the K -theory. The turbulent momentum flux can be rewritten as

$$\overline{u'w'} = -K \frac{\partial \bar{u}}{\partial z}, \tag{8}$$

where K is the turbulent transfer coefficient (m² s⁻¹), which is a physical parameter representing the capacity of the airflow to transfer momentum (Shao, 2008). The value of K can be obtained from $\overline{u'w'}$ derived from Eq. 6 and the measured wind velocity profile.

RESULTS AND DISCUSSION

Drag Coefficient and Roughness Length Over Gravel Surfaces

We measured the drag coefficient C_D at gravel coverages of 0, 5, 10, 15, 20, 25, and 30% under wind speeds of 6, 8, and 10 m s⁻¹ (Figure 5). The C_D over a flat sand surface (0%) ranged from 0.0021 to 0.0024, with an average value of 0.0023, which is close to that which Dong Z. et al. (2002) measured in another wind tunnel experiments (= 0.0028).

The variations in C_D were dependent on gravel coverage. Values of C_D over fine-grained gravel surfaces ranged from 0.0023 to 0.0036 (average was 0.0029, SD was 0.0005), 1–1.7 times those on flat sand surface (Figure 5). C_D increased substantially as coverage increased from 5 to 15%, showing a peak at 15% gravel coverage. At 20% gravel coverage, C_D dropped to close to the level at 0% coverage. With increasing gravel coverage greater than 20%, C_D increased slightly. The resistance to airflow was greatest at the gravel coverage of 15%, and the effect of rough surface on airflow tends to stabilize at gravel coverages of 20% and greater. Marshall (1971) proposed that airflow over gravel surfaces is influenced by drag generated by the gravel and the intervening surface between the gravel pebbles. Although the size of fine-grained gravels is small, the surface can be considered to be dynamically rough. Here, we calculated the roughness elements Reynolds number, which is a

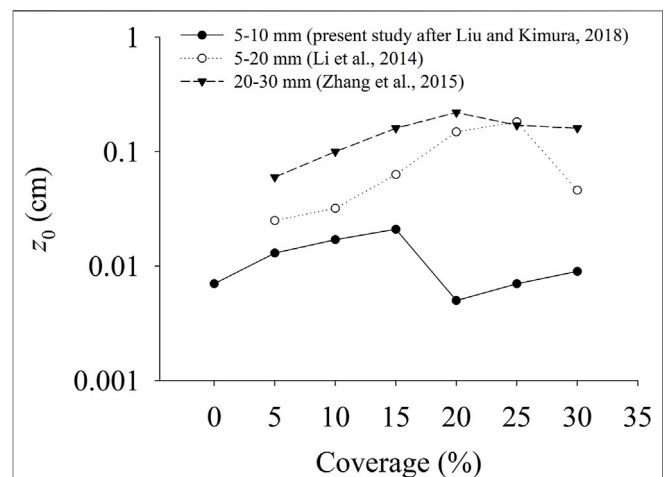
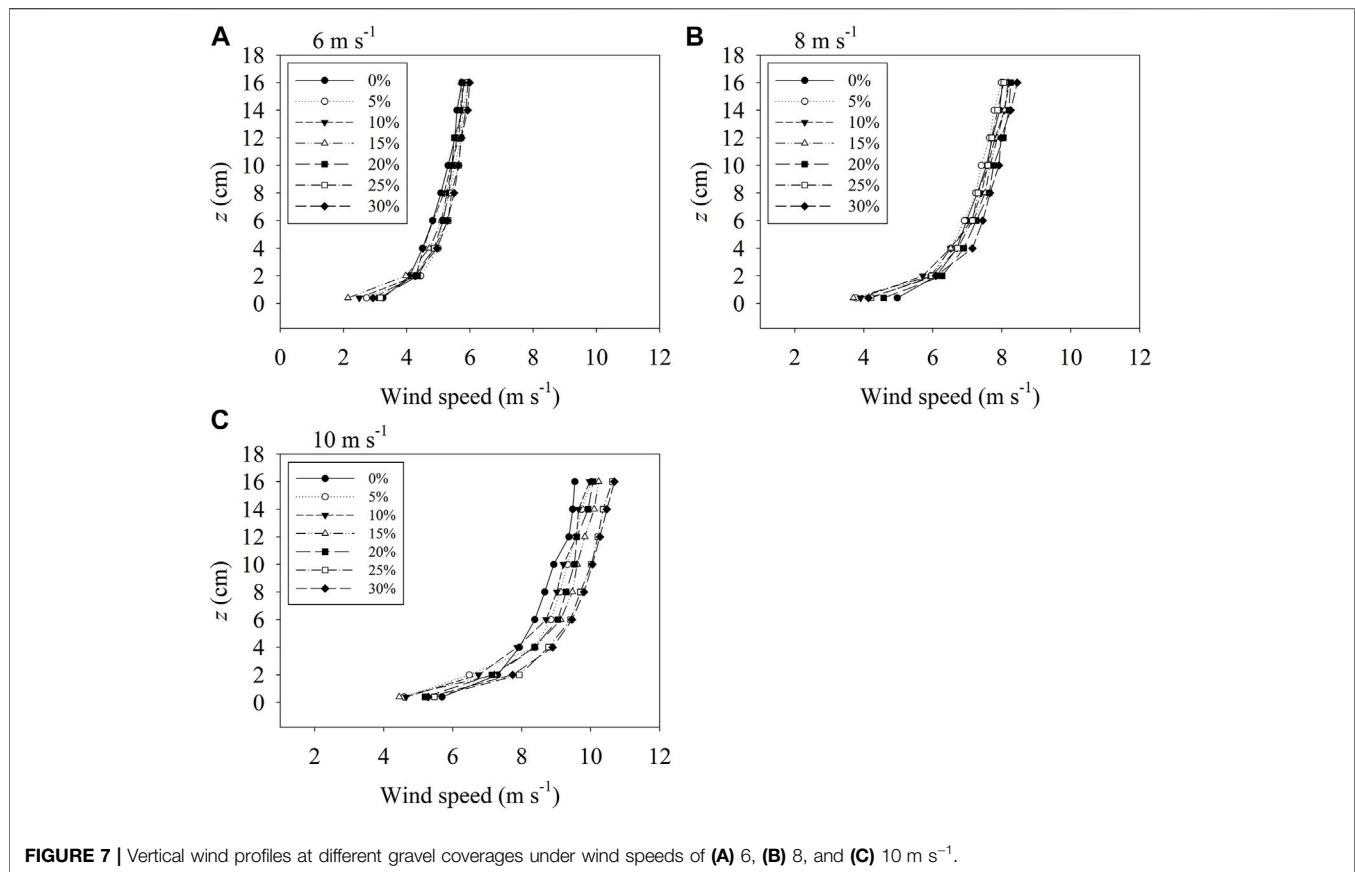


FIGURE 6 | Comparison of average roughness length z_0 at different gravel coverages from Liu and Kimura (2018) with other published data from Li et al. (2014) and Zhang et al. (2015).



criterion to determine whether a surface is rough (>300) or smooth (<300). The roughness elements Reynolds number is defined as $Re_r = u_* D_r / \nu$, where D_r is the typical roughness-element size, and ν is the kinematical molecular viscosity and is approximately $1.5 \times 10^{-5} \text{ m}^2 \text{ s}^{-1}$ for atmospheric boundary-layer flows (Shao, 2008). The value of Re_r for the fine-grained gravel surfaces exceeded 300, indicating that our tested surfaces were rough to affect the airflow. Considering fine-grained gravel as an isolated roughness element, when gravel coverage increases to a threshold value, the intervening surface is protected by individual gravel pebbles and will not resist airflow. Previous studies (Lee and Soliman, 1977; Raupach, 1992; Liu and Kimura, 2018) have pointed out that gravel surfaces become physically and aerodynamically smooth at a threshold coverage where roughness length drops off after the peak value. We infer that over stable gravel surfaces (i.e., 20% coverage), newly added gravel will be protected by existing gravel; as a result, C_D approximates to that of flat sand surface (0% coverage).

Aerodynamically, the increase of resistance force (drag coefficient) over the gravel surface is associated with the increased surface roughness length, which increases the contact area between the ground surface and airflow. Roughness length z_0 over gravel surfaces was 1.2–3 times that of flat sand surface, depending on gravel coverage (Figure 6). The variations in z_0 and C_D with the change of gravel coverage followed a similar trend, i.e., their values reached a peak at 15% coverage and decreased at 20%

coverage to the level comparable to that on the flat sand surface. We compared our experimental results for z_0 , as previously published (Liu and Kimura, 2018), with other published data to clarify the effects of gravel coverage on roughness length (Figure 6). Generally, ground surfaces covered by larger pebbles tend to have greater roughness lengths. Li et al. (2014) and Zhang et al. (2015) found in wind tunnel experiments that the values of z_0 appeared to peak at 25 and 20% coverage with pebble sizes of 5–20 mm and 20–30 mm, respectively. The variation of z_0 in our experiment is consistent with the results of Li et al. (2014) and Zhang et al. (2015) but showed smaller values resulting from smaller pebble size (5–10 mm).

Wind-Speed Gradient Over Gravel Surfaces

On a flat sand surface, the vertical wind profile increases logarithmically with increasing height. The logarithmic law was also confirmed for the vertical distribution of wind speed over gravel surfaces (Figure 7). As wind speed increased, the effect of gravel surfaces on wind profile became more obvious. At each wind speed, wind speed on the flat sand surface was larger than those over gravel surfaces at a height of 0.4 cm, showing a wind-reduction effect even over surfaces covered by pebbles. Specially, wind speed was the lowest at 15% coverage because of the greatest drag force generated by gravels and the intervening surface (Figure 5). This result indicated that gravel surface at 15% coverage had the best wind-reduction effect.

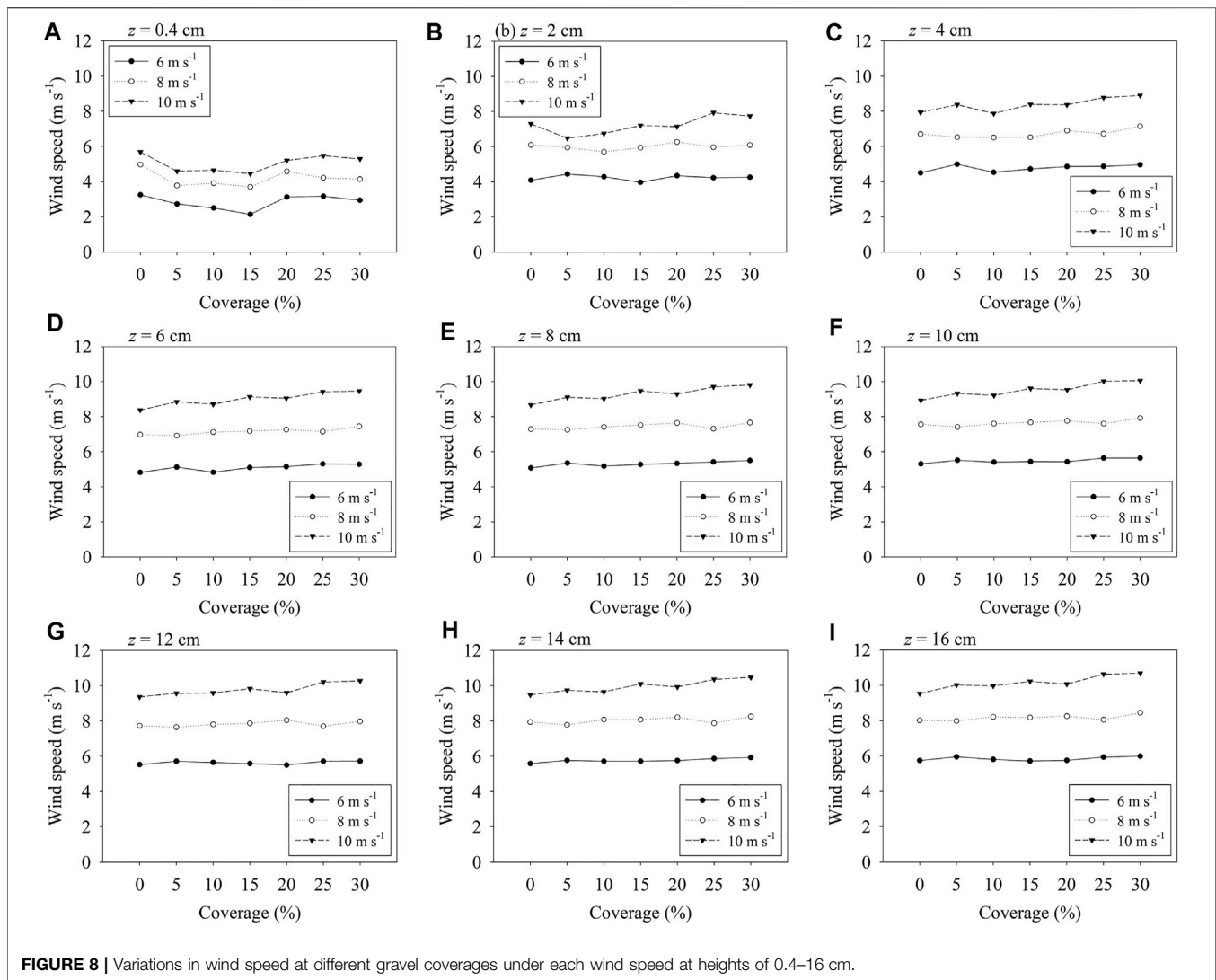


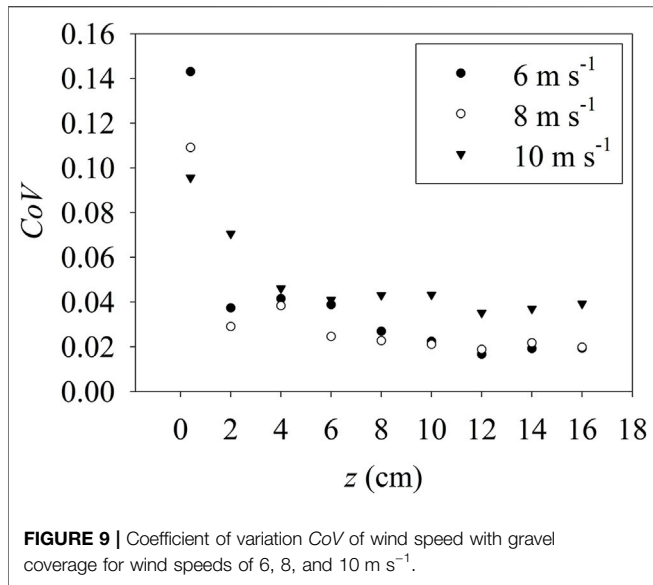
FIGURE 8 | Variations in wind speed at different gravel coverages under each wind speed at heights of 0.4–16 cm.

To visualize the wind speed fluctuations more clearly, we compared variations of wind speed at different gravel coverages at each height (**Figure 8**). At a height of 0.4 cm, which is below the average height of the gravel, wind speed varied greatly with the increase in gravel coverage, showing an opposite trend to that of roughness length (**Figure 8A**). At gravel coverage of 20% and greater, wind speed tended to be uniform. At a height of 2 cm (about two to four times pebble size), the variation of wind speed differed at each wind speed but tended to stabilize at gravel coverage of 25% and greater. (**Figure 8B**). In contrast to the wind speed variations at heights below 4 cm, those at heights of 4 cm and above were relatively stable (**Figures 8C–I**).

Because of the presence of gravel, airflow near the ground surface in our compact wind tunnel was characterized by two sublayers. The layer below a height of 4 cm was defined as the roughness sublayer, in which airflow was influenced strongly by individual gravel, and the wind speed varied complexly. The layer above 4 cm was defined as the inertial sublayer, where airflow was

dominated by the characteristics of the entire gravel bed, and the wind speed varied regularly with gravel coverage. Tan et al. (2012) used large pebbles (2–3 cm) at gravel coverages of 5–80% in wind-tunnel experiments and found that wind speed distribution near the ground surface can be divided clearly into two layers at the height of 2.2 cm. However, because of the different pebble sizes, wind speed decreased as coverage increased from 5 to 35% and tended to be uniform at coverages of 40–80%.

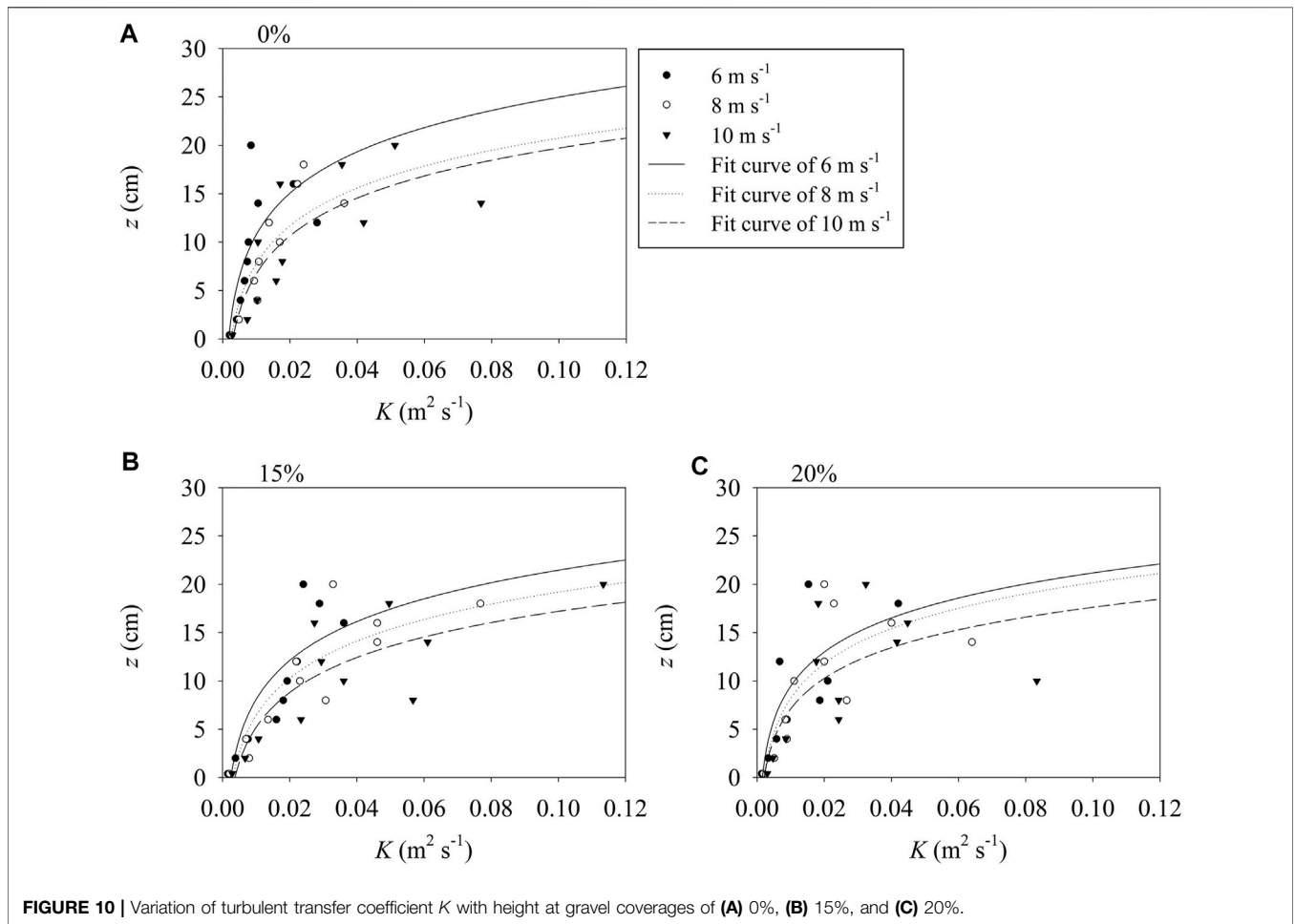
Variation in gravel surface coverage affects the characteristics of the near-ground surface wind profile and thus affects the structural characteristics of wind-blown sand flux (Wu, 1987). CoV of wind speed with gravel coverage differed with height (**Figure 9**). CoV values were higher in the roughness sublayer (below 4 cm), about 2.7–8.6 times those in the inertial sublayer (above 4 cm), indicating that wind-speed fluctuations are more likely to be affected by the variation in gravel coverage in the roughness sublayer. In the inertial sublayer, wind-speed fluctuation is influenced less by gravel coverage and tended to stabilize. The influence of gravel coverage on wind-speed



fluctuation decreased with increasing height, showing notable differences below and above 4 cm, which is the threshold between the roughness sublayer and the inertial sublayer. At the height of 4 cm, approximate CoV values were observed under each wind speed, indicating that wind-speed fluctuation was independent of changes in gravel coverage. The threshold height of 4 cm was in accordance with that defined as the equilibrium point of vertical profiles of wind-blown sand flux over gravel surfaces in our previous study, in which characteristic of blown sand flux was independent of both wind speed and gravel coverage (Liu et al., 2020).

Turbulent Structure Over Gravel Surface

The turbulent transfer coefficient K is a parameter used to quantify the capacity of the flow to transfer momentum through turbulent mixing. To investigate the effect of fine-grained gravel surfaces on the vertical structure of turbulence, we compared the variation of K with height on the flat sand surface (0%) and over gravel surfaces with 15 and 20% coverage at



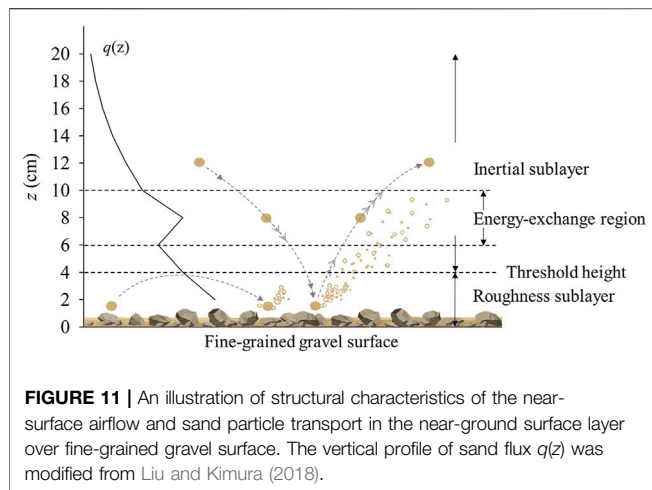


FIGURE 11 | An illustration of structural characteristics of the near-surface airflow and sand particle transport in the near-ground surface layer over fine-grained gravel surface. The vertical profile of sand flux $q(z)$ was modified from Liu and Kimura (2018).

wind speeds of 6, 8, and 10 m s⁻¹ (Figure 10). Here, we discuss only those two coverages where drag coefficient (Figure 5) and roughness length (Figure 6) reached peak and dropped to the minimum. Over the flat sand surface and the fine-grained gravel surface (15 and 20% coverage), K increased with height (Figure 10), which is consistent with the observations of Stull (2012) and Lu and Dong (2006). The reason for this increase is that turbulence intensity near the ground surface was greatest because of the friction force of the ground. However, that is also the region of maximum turbulent energy dissipation. The interactions between turbulence intensity and turbulent energy dissipation resulted in a weaker energy exchange between the turbulent kinetic energy and momentum. The farther from the surface, the more effective the energy exchange was.

We compared the values of K at each height for different surfaces. We found that the values of K over gravel surfaces were close to those on the sand surface, indicating that the fine-grained gravel surface has little effect on the turbulent energy exchange below 4 cm height, which corresponded to the range of roughness sublayer. Above 4 cm (i.e., inertial sublayer), values of K at gravel coverages of 15 and 20% were obviously higher at heights of 6–10 cm, reaching a maximum of about 3 times that of the flat sand surface. As height increased above 10 cm, the difference in K became smaller, while values of K over gravel surfaces were still slightly higher. Moreover, we also found that at the gravel coverage of 15 and 20%, the average values of K at heights between 6 and 10 cm are 11.8 and 9.5 times than those at 0.4 cm, respectively. The comparison results of K were consistent with the mixing length hypothesis that K is proportional to height (Shao, 2008).

Our findings show that when the roughness sublayer transitioned to the inertial sublayer, a region of more effective energy exchange formed at heights of 6–10 cm, which we defined as the energy-exchange region (Figure 11). We suggest that this structural characteristic helps to clarify the mechanism of wind-blown sand transport over fine gravel surfaces. During wind-blown sand transport, saltation particles are lifted a short distance above the surface and absorb kinetic energy from the airflow. When these particles hit the ground, they eject more particles into the

air, initiating an increase in the number of airborne particles and hence in blown sand flux (Shao, 2008). Over gravel surfaces, saltation particles and bounced particles gain more energy when they transport through the energy-exchange region. Those saltation particles would impact the ground with an accelerating velocity and the bounced particles might be transported higher or farther. Our previous findings have demonstrated that wind-blown sand at all tested coverages of fine gravel (5–30%) maintains an erosional state (Liu et al., 2020); this result might be explained by formation of an energy-exchange region within the turbulent structure.

In an investigation of vertical profiles of sand flux over fine-grained gravel surfaces, Liu and Kimura (2018) found that a strong peak in blown sand flux appeared at a height of 8 cm when gravel coverage reached 20% (Figure 12). Liu and Kimura (2018) inferred that the peak resulted from the fact that sand particles bounce higher after collisions. We found that the local maximum sand flux occurred at a height in the range of the energy-exchange region (6–10 cm) observed in the current study, where blown sand particles absorb the momentum transferred from turbulent kinetic energy. However, a local maximum blown sand flux at 8 cm was not observed for gravel coverage of 15%; the lack of this local maximum is because C_D reached a maximum at 15% gravel coverage (Figure 5). Gravels and the intervening surface hinder erosion and trap wind-blown sand thus effectively inhibit wind-blown sand. Aerodynamic characteristics of the near-surface airflow explains how fine-grained gravel surfaces affect the vertical structure of blown sand flux at different coverages.

CONCLUSION

In this study, we examined the effect of gravel coverage (0–30%) on the drag coefficient C_D , wind-speed gradient, and turbulent transfer coefficient K in a compact boundary-layer wind-tunnel with a turbulence generator at wind speeds of 6, 8, and 10 m s⁻¹. We tested fine-grained gravels with pebble sizes typical of the southern Gobi Desert, the main source of Asian Dust. Our findings are as follows:

- 1) The response of airflow to the gravel surface are characterized quantitatively by C_D . At gravel coverages of 0–15%, C_D increased with increasing coverage because airflow over the gravel surface was disturbed by drag generated by the gravel and the intervening surface. The drag force was greatest when gravel coverage reached 15%. At coverage of 20% or greater, the intervening surface did not generate drag because of protection by the individual gravel pebbles.
- 2) The wind profile near the ground surface was divided into two layers that varied in response to the different characteristics of the wind-speed gradient with gravel coverage: the roughness sublayer below 4 cm and the inertial sublayer above 4 cm. The variation of the wind speed with gravel coverage was more complex in the roughness sublayer but was more uniform in the inertial sublayer. At the height of 4 cm, wind-speed fluctuations were independent of changes in gravel coverage under the observed wind speeds.

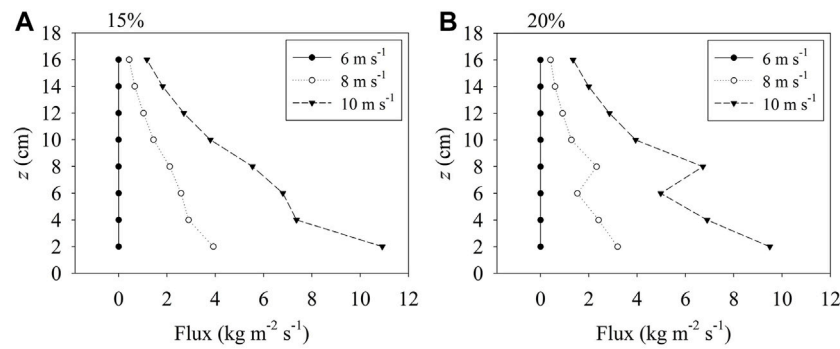


FIGURE 12 | Vertical profiles of sand flux under wind speeds of 6, 8, and 10 m s^{-1} at gravel coverages of **(A)** 15 and **(B)** 20% [modified from Liu and Kimura (2018)].

3) An energy-exchange region, where sand particles can absorb more energy from the surrounding airflow, might be existed between the roughness sublayer and the inertial sublayer over the fine-grained gravel surfaces. In this region, the most effective transfer of energy appeared at 15% gravel coverage, with a maximum of 3 times the value of K at the same height over the sand surface compared to that over the sand surface without gravel.

Our results provide additional information about the effect of various coverages of fine gravel on wind-speed characteristics near the ground surface. Our findings can be applied to determine the aerodynamic stability of the gobi surface and to provide a reference for elucidation of the structural characteristics of windblown sand flux. Although the wind tunnel reproduced natural surface conditions and the 34-cm boundary layer, the height of the equilibrium point and the range of the energy-exchange region between the roughness sublayer and the inertial sublayer are required to validate field observations. If these variables can be determined in wind tunnels, then we will be able to estimate the wind profile over gravel surfaces

accurately and thus improve the accuracy of wind-erosion prediction models.

DATA AVAILABILITY STATEMENT

The raw data supporting the conclusion of this article will be made available by the authors, without undue reservation.

AUTHOR CONTRIBUTIONS

JL and RK contributed to conception of the start. JL and JW contributed to data analysis and wrote the first draft of the manuscript. All authors contributed to manuscript revision, read, and agreed to the published version of the manuscript.

FUNDING

This study was supported by Japan Society for the Promotion of Science KAKENHI Grant Numbers 19H04239 and 21K17880.

REFERENCES

- Bagnold, R. A. (2012). *The Physics of Blown Sand and Desert Dunes*. London: Courier Corporation.
- Bian, H., Tie, X., Cao, J., Ying, Z., Han, S., and Xue, Y. (2011). Analysis of a Severe Dust Storm Event over China: Application of the WRF-Dust Model. *Aerosol Air Qual. Res.* 11 (4), 419–428. doi:10.4209/aaqr.2011.04.0053
- Butterfield, G. R. (1999). Near-Bed Mass Flux Profiles in Aeolian Sand Transport: High-Resolution Measurements in a Wind Tunnel. *Earth Surf. Process. Landforms* 24 (5), 393–412. doi:10.1002/(sici)1096-9837(199905)24:5<393:aid-esp996>3.0.co;2-g
- Cosseron, A., Gunturu, U. B., and Schlosser, C. A. (2013). Characterization of the Wind Power Resource in Europe and its Intermittency. *Energ. Proced.* 40, 58–66. doi:10.1016/j.egypro.2013.08.008
- Darmenova, K., Sokolik, I. N., Shao, Y., Marticorena, B., and Bergametti, G. (2009). Development of a Physically Based Dust Emission Module within the Weather Research and Forecasting (WRF) Model: Assessment of Dust Emission Parameterizations and Input Parameters for Source Regions in Central and East Asia. *J. Geophys. Res.-Atmos.* 114 (D14). doi:10.1029/2008JD011236
- Dong, Z. B., Liu, X. P., and Wang, X. M. (2002a). Aerodynamic Roughness of Gravel Surfaces. *Geomorphology* 43 (1-2), 17–31. doi:10.1016/S0169-555x(01)00097-6
- Dong, Z., Qu, J., Liu, X., Zhang, W., and Wang, X. (2002b). Experimental Investigation of Drag Coefficients of Gobi Surfaces. *Sci. China Ser. D-earth Sci.* 45 (7), 609–615. doi:10.1360/02yd9062
- Frank, A., and Kocurek, G. (1994). Effects of Atmospheric Conditions on Wind Profiles and Aeolian Sand Transport with an Example from white Sands National monument. *Earth Surf. Process. Landforms* 19 (8), 735–745. doi:10.1002/esp.3290190806
- Friedman, G. M., and Sanders, J. E. (1978). *Principles of Sedimentology*. New York: Wiley.
- Garratt, J. R. (1994). The Atmospheric Boundary-Layer - Review. *Earth-sci. Rev.* 37 (1-2), 89–134. doi:10.1016/0012-8252(94)90026-4
- Irwin, H. P. A. H. (1981). The Design of Spires for Wind Simulation. *J. Wind Eng. Ind. Aerodyn.* 7 (3), 361–366. doi:10.1016/0167-6105(81)90058-1
- Jensen, M., and Franck, N. (1963). *Model-scale Tests in Turbulent Wind: Part 2*. Copenhagen: Danish Technical Press.
- Jensen, M. (1958). The Model-Law for Phenomena in Natural Wind. *Ingenioren* 2 (2), 121–128.

- Lee, B. E., and Soliman, B. F. (1977). An Investigation of the Forces on Three Dimensional bluff Bodies in Rough wall Turbulent Boundary Layers. *J. Fluids Eng.* 99 (3), 503–509. doi:10.1115/1.3448828
- Li, G. S., Qu, J. J., Li, X. Z., and Wang, W. F. (2014). The Sand-Deposition Impact of Artificial Gravel Beds on the protection of the Mogao Grottoes. *Sci. Rep.* 4 (1), 4341–4348. ARTN 434110. doi:10.1038/srep04341
- Liu, J. Q., and Kimura, R. (2017a). Development of a Method to Make a Boundary Layer with Roughness Length Close to Natural Conditions in a Simple Wind Tunnel. *Sand Dune Res.* (64), 1–8.
- Liu, J. Q., and Kimura, R. (2017b). Study on the Boundary Layer Formation of a Small Simple Type Wind Tunnel. *Sand Dune Res.* 63 (3), 113–119.
- Liu, J., and Kimura, R. (2018). Wind Speed Characteristics and Blown Sand Flux over a Gravel Surface in a Compact Wind Tunnel. *Aeolian Res.* 35, 39–46. doi:10.1016/j.aeolia.2018.09.005
- Liu, J., Kimura, R., and Wu, J. (2020). Vertical Profiles of Wind-Blown Sand Flux over fine Gravel Surfaces and Their Implications for Field Observation in Arid Regions. *Atmosphere* 11 (10), 1029. doi:10.3390/atmos11101029
- Lü, P., and Dong, Z. (2006). Wind Tunnel Experiments on the Turbulent Transmission over the Near Surface Layer of Different Surfaces. *Environ. Geol.* 50 (7), 983–988. doi:10.1007/s00254-006-0267-4
- Marshall, J. K. (1971). Drag Measurements in Roughness Arrays of Varying Density and Distribution. *Agric. Meteorol.* 8, 269–292. doi:10.1016/0002-1571(71)90116-6
- Marticorena, B., Bergametti, G., Gillette, D., and Belnap, J. (1997). Factors Controlling Threshold Friction Velocity in Semiarid and Arid Areas of the United States. *J. Geophys. Res.* 102 (D19), 23277–23287. doi:10.1029/97jd01303
- Niu, J.-q., Zhou, D., and Liang, X.-f. (2017). Experimental Research on the Aerodynamic Characteristics of a High-Speed Train under Different Turbulence Conditions. *Exp. Therm. Fluid Sci.* 80, 117–125. doi:10.1016/j.expthermflusci.2016.08.014
- Raupach, M. R. (1992). Drag and Drag Partition on Rough Surfaces. *Boundary-layer Meteorol.* 60 (4), 375–395. doi:10.1007/Bf00155203
- Shao, Y. P. (2008). *Physics and Modelling of Wind Erosion*, 37. Dordrecht: Springer Science & Business Media.
- Sharp, R. P. (1980). Wind-driven Sand in Coachella Valley, California: Further Data. *Geol. Soc. America Bull.* 91 (12), 7242–7730. doi:10.1130/0016-7606(1980)91<7242:wsicvc>2.0.co;2
- Stull, R. B. (2012). *An Introduction to Boundary Layer Meteorology*, 13. Dordrecht: Springer Science & Business Media.
- Tan, L. H., Zhang, W. M., An, Z. S., and Li, J. G. (2012). Response of Wind Velocity Gradient at Boundary Layer to Gravel Coverage. *J. Desert Res.* (6), 3.
- Tan, L., Zhang, W., Liu, B., An, Z., and Li, J. (2013). Simulation of Wind Velocity Reduction Effect of Gravel Beds in a mobile Wind Tunnel Atop the Mogao Grottoes of Dunhuang, China. *Eng. Geology.* 159, 67–75. doi:10.1016/j.enggeo.2013.03.015
- Wu, Z. (1987). *Aeolian Geomorphology*. Beijing: Science Press.
- Zhang, W., Tan, L., Zhang, G., Qiu, F., and Zhan, H. (2014). Aeolian Processes over Gravel Beds: Field Wind Tunnel Simulation and its Application Atop the Mogao Grottoes, China. *Aeolian Res.* 15, 335–344. doi:10.1016/j.aeolia.2014.07.001
- Zhang, K., Zhang, W., Tan, L., An, Z., and Zhang, H. (2015). Effects of Gravel Mulch on Aeolian Transport: a Field Wind Tunnel Simulation. *J. Arid Land* 7 (3), 296–303. doi:10.1007/s40333-015-0121-1

Conflict of Interest: The authors declare that the research was conducted in the absence of any commercial or financial relationships that could be construed as a potential conflict of interest.

Publisher's Note: All claims expressed in this article are solely those of the authors and do not necessarily represent those of their affiliated organizations, or those of the publisher, the editors and the reviewers. Any product that may be evaluated in this article, or claim that may be made by its manufacturer, is not guaranteed or endorsed by the publisher.

Copyright © 2021 Liu, Kimura and Wu. This is an open-access article distributed under the terms of the Creative Commons Attribution License (CC BY). The use, distribution or reproduction in other forums is permitted, provided the original author(s) and the copyright owner(s) are credited and that the original publication in this journal is cited, in accordance with accepted academic practice. No use, distribution or reproduction is permitted which does not comply with these terms.